Author(s): Tuovinen, Toni & Hinkkanen, Marko & Harnefors, Lennart & Luomi, Jorma

Title: A reduced-order position observer with stator-resistance adaptation for synchronous reluctance motor drives

Year: 2010

Version: Post print

Please cite the original version:

Tuovinen, Toni & Hinkkanen, Marko & Harnefors, Lennart & Luomi, Jorma. 2010. A reduced-order position observer with stator-resistance adaptation for synchronous reluctance motor drives. 2010 14th International Power Electronics and Motion Control Conference (EPE/PEMC). 6. ISBN 978-1-4244-7856-9 (electronic). DOI: 10.1109/epepemc.2010.5606645.

A Reduced-Order Position Observer with Stator-Resistance Adaptation for Synchronous Reluctance Motor Drives

Toni Tuovinen*, Marko Hinkkanen*, Lennart Harnefors†, and Jorma Luomi*
*Aalto University School of Science and Technology
Department of Electrical Engineering, P.O. Box 13000, FI-00076 Aalto, Finland
†ABB Power Systems, PSDC/DCTU, SE-77180 Ludvika, Sweden

***Abstract*—A reduced-order position observer with stator-resistance adaptation is applied for motion-sensorless synchronous reluctance motor drives. A general analytical solution for the stabilizing observer gain and stability conditions for the stator-resistance adaptation are given. The local stability of the position and stator-resistance estimation is guaranteed at every operating point except the zero frequency, if inductances are known accurately. The observer design is experimentally tested using a 6.7-kW synchronous reluctance motor drive; stable operation at low speeds under various loading conditions is demonstrated.**

***Index Terms*—Observer, stability conditions, speed sensorless, stator resistance estimation.**

I. Introduction

The torque production in synchronous reluctance motors (SyRMs) is based on the magnetic saliency of the rotor. The absence of the rotor winding (and the rotor current) may reduce the losses of SyRMs as compared to induction motors [1]. Due to simpler structure and smaller energy losses, modern SyRMs are feasible competitors for induction motors in variable-speed drives [2], [3].

The rotor position of a SyRM has to be known with good accuracy in order to obtain stable operation and high performance. The rotor position can be either measured or estimated. Motion-sensorless control is usually preferable: speed sensors are expensive, they can be damaged or, in some environments and applications, cannot be installed. Furthermore, sensorless control ensures the operation of the drive equipped with a motion sensor in cases the sensor is damaged.

In low-cost applications, motion-sensorless operation of the drive is preferred, and signal-injection methods should be avoided in order to minimize hardware costs. Hence, a robust and easy-to-tune rotor-position observer, based only on the fundamental excitation, is needed [4], [2].

Motion-sensorless AC drives may have unstable operating regions at low speeds. The back electromotive force (EMF) is proportional to the rotational speed of the motor. At low speeds, the back EMF becomes weak and the observer becomes increasingly sensitive to parameter errors [5]. In practice, the stator resistance varies with the winding temperature during the operation of the motor, and AC motors are usually magnetically saturated in the rated operating point. Even if the motor parameters are accurately known, improper observer gain selections may cause unstable operation of the drive [6], [7].

Usually, an in-depth stability analysis of position estimation methods is omitted since the resulting closed-loop systems become increasingly complicated as the order of the observer increases. Hence, a low order is an attractive design goal for rotor-position observers.

To extend the range of stable operation to low speeds, including zero speed, methods incorporating additional current or voltage signal have been proposed [8], [9]. Other speed and position estimation methods exploit modified PWM [10], [11], for example. In some applications, a position observer can be augmented with a signal-injection method for low-speed operation [12].

In this paper, the reduced-order proposed in [13] for permanent magnet synchronous motor drives is applied for a SyRM drive. The observer is augmented with the stator-resistance adaptation in low-speed operation. With accurate inductance estimates, the linearized closed-loop system is stable in every operation point, except the zero frequency. The performance of the observer design is evaluated using laboratory experiments with a 6.7-kW SyRM drive. For improved low-speed operation, the observer could be augmented with a signal-injection method, for example in a fashion similar to [14].

II. SyRM Model

Real space vectors will be used here. For example, the stator-current vector is $\boldsymbol{i}_\mathrm{s} = [i_\mathrm{d}, i_\mathrm{q}]^\mathrm{T}$, where i_d and i_q are the components of the vector and the matrix transpose is marked with the superscript T. The orthogonal rotation matrix is defined as

$$\mathbf{I} = \begin{bmatrix} 1 & 0 \\ 0 & 1 \end{bmatrix}$$

respectively. Since $\mathbf{J}$ corresponds to the imaginary unit j, the notation is very similar to that obtained for complex space vectors.

The electrical position of the d axis is denoted by ϑ_m. The d axis is defined as the direction of the maximum inductance of the rotor. The position depends on the electrical angular rotor speed ω_m according to

$$\frac{\mathrm{d}\vartheta_\mathrm{m}}{\mathrm{d}t} = \omega_\mathrm{m} \tag{1a}$$

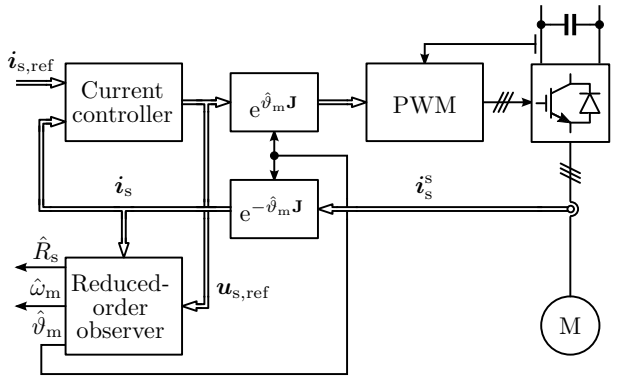

Fig. 1. Motion-sensorless rotor-oriented controller. The observer is implemented in the estimated rotor coordinates.

To simplify the analysis in the following sections, the machine model will be expressed in the *estimated* rotor reference frame, whose d axis is aligned at $\hat{\vartheta}_\mathrm{m}$ with respect to the stator reference frame. The stator inductance is

$$\boldsymbol{L} = \mathrm{e}^{-\tilde{\vartheta}_\mathrm{m}\mathbf{J}} \begin{bmatrix} L_\mathrm{d} & 0 \\ 0 & L_\mathrm{q} \end{bmatrix} \mathrm{e}^{\tilde{\vartheta}_\mathrm{m}\mathbf{J}} \tag{1b}$$

where $\tilde{\vartheta}_\mathrm{m} = \hat{\vartheta}_\mathrm{m} - \vartheta_\mathrm{m}$ is the estimation error in the rotor position, L_d the direct-axis inductance, and L_q the quadrature-axis inductance. The voltage equation is

$$\frac{\mathrm{d}\boldsymbol{\psi}_\mathrm{s}}{\mathrm{d}t} = \boldsymbol{u}_\mathrm{s} - R_\mathrm{s}\boldsymbol{i}_\mathrm{s} - \hat{\omega}_\mathrm{m}\mathbf{J}\boldsymbol{\psi}_\mathrm{s} \tag{1c}$$

where $\boldsymbol{\psi}_\mathrm{s}$ is the stator-flux vector, $\boldsymbol{u}_\mathrm{s}$ the stator-voltage vector, R_s the stator resistance, and $\hat{\omega}_\mathrm{m} = \mathrm{d}\hat{\vartheta}_\mathrm{m}/\mathrm{d}t$ is the angular speed of the coordinate system. The stator current is a nonlinear function

$$\boldsymbol{i}_\mathrm{s} = \boldsymbol{L}^{-1}\boldsymbol{\psi}_\mathrm{s} \tag{1d}$$

of the stator-flux vector and the position error $\tilde{\vartheta}_\mathrm{m}$.

III. Rotor-Position Observer

The observer in estimated rotor coordinates is considered. A typical rotor-oriented control system is depicted in Fig. 1. Accurate parameter estimates L_d and L_q are assumed.[1]

A. Structure

The observer proposed in [13] is based on estimating the d component $\hat{\psi}_\mathrm{d}$ of the stator flux and the rotor position. The componentwise presentation of the observer is

$$\frac{\mathrm{d}\hat{\psi}_\mathrm{d}}{\mathrm{d}t} = u_\mathrm{d} - \hat{R}_\mathrm{s} i_\mathrm{d} + \hat{\omega}_\mathrm{m} L_\mathrm{q} i_\mathrm{q} + k_1(\hat{\psi}_\mathrm{d} - L_\mathrm{d} i_\mathrm{d}) \tag{2a}$$

$$\frac{\mathrm{d}\hat{\vartheta}_\mathrm{m}}{\mathrm{d}t} = \frac{u_\mathrm{q} - \hat{R}_\mathrm{s} i_\mathrm{q} - L_\mathrm{q}\frac{\mathrm{d}i_\mathrm{q}}{\mathrm{d}t} + k_2(\hat{\psi}_\mathrm{d} - L_\mathrm{d} i_\mathrm{d})}{\hat{\psi}_\mathrm{d}} \tag{2b}$$

where k_1 and k_2 are observer gain parameters. The rotor speed estimate is obtained directly from (2b) since $\hat{\omega}_\mathrm{m} = \mathrm{d}\hat{\vartheta}_\mathrm{m}/\mathrm{d}t$. The observer is of the second order and there are only two gains.

[1]In practical implementations, the effect of the magnetic saturation on L_d and L_q can be taken into account using explicit functions or look-up tables.

B. Stabilizing Observer Gain

The gains k_1 and k_2 determine the stability (and other properties) of the observer. The closed-loop system consisting of (1) and (2) is locally stable in every operating point if the gains are given by

$$k_1 = -\frac{b + \beta(c/\hat{\omega}_\mathrm{m} - \hat{\omega}_\mathrm{m})}{\beta^2 + 1}, \quad k_2 = \frac{\beta b - c/\hat{\omega}_\mathrm{m} + \hat{\omega}_\mathrm{m}}{\beta^2 + 1} \tag{3}$$

where the coefficients $b > 0$ and $c > 0$ may depend on the operating point[2] and

$$\beta = \frac{i_\mathrm{q}}{i_\mathrm{d}} \tag{4}$$

The observer gain design problem is reduced to the selection of the two positive coefficients b and c, which are actually the coefficients of the characteristic polynomial of the linearized closed-loop system. Hence, (3) can be used to place the poles of the linearized closed-loop system arbitrarily. In (3), an accurate stator-resistance estimate $\hat{R}_\mathrm{s}$ is assumed. This assumption will be lifted in Section III-C.

The stability with accurate parameter estimates is necessary but not a sufficient design goal. In addition, it is typically required that the system should be well damped, robust against parameter errors and noise, and easy to tune. Based on numerical studies, the coefficient b in (3) can be kept constant while $c = b|\hat{\omega}_\mathrm{m}| + \hat{\omega}_\mathrm{m}^2$ leads to the simple gains [13]

$$k_1 = -b\frac{\beta\,\mathrm{sign}(\hat{\omega}_\mathrm{m}) + 1}{\beta^2 + 1}, \quad k_2 = b\frac{\beta - \mathrm{sign}(\hat{\omega}_\mathrm{m})}{\beta^2 + 1} \tag{5}$$

that are independent on the rotor speed estimate (except its sign). This gain selection is an acceptable compromise between design criteria (damping, robustness, and simplicity). If different design criteria are preferred, coefficients b and c could be determined by pole placement or searched by means of numerical optimization, for example.

C. Stator-Resistance Adaptation

The stator resistance adaptation law proposed in [13] is

$$\frac{\mathrm{d}\hat{R}_\mathrm{s}}{\mathrm{d}t} = k_\mathrm{R}(\hat{\psi}_\mathrm{d} - L_\mathrm{d} i_\mathrm{d}) \tag{6}$$

where k_R is the adaptation gain. The general stability conditions for the observer augmented with (6) are

$$k_\mathrm{R} i_\mathrm{q} \hat{\omega}_\mathrm{m} > 0 \tag{7a}$$

$$k_\mathrm{R}[(i_\mathrm{d} - \beta i_\mathrm{q})b - 2 i_\mathrm{q}\hat{\omega}_\mathrm{m}] + bc > 0 \tag{7b}$$

where b and c are the positive design parameters in (3).

Based on the condition (7a), the sign of the gain k_R has to depend on the operating mode. Furthermore, the magnitude of k_R has to be limited according to (7b). It can be shown that the conditions in (7) are fulfilled by choosing

$$k_\mathrm{R} = \begin{cases} \min\{k'_\mathrm{R}, L\}, & \text{if } i_\mathrm{q}\hat{\omega}_\mathrm{m} > 0 \text{ and } L > 0 \\ \max\{-k'_\mathrm{R}, L\}, & \text{if } i_\mathrm{q}\hat{\omega}_\mathrm{m} < 0 \text{ and } L < 0 \\ k'_\mathrm{R}\,\mathrm{sign}(i_\mathrm{q}\hat{\omega}_\mathrm{m}), & \text{otherwise} \end{cases} \tag{8}$$

[2]For $\hat{\omega}_\mathrm{m} = 0$, $c = 0$ has to be selected to avoid division by zero, giving only marginal stability for zero speed.

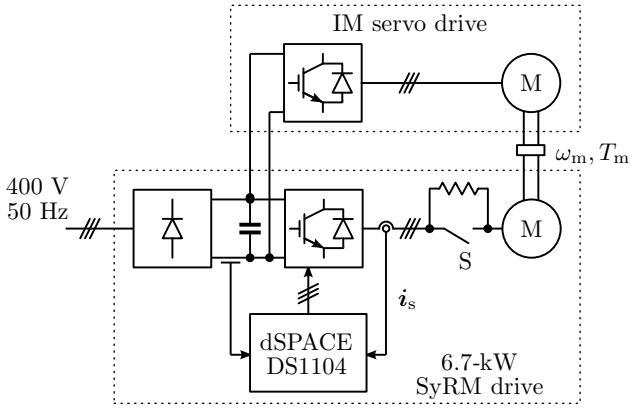

Fig. 2. Experimental setup. The stator currents and the DC-link voltage are used as feedback signals. Mechanical load is provided by a servo drive. The shaft torque T_m and the rotor speed ω_m are measured for monitoring purposes. Three-phase switch S is in the closed position, except in the experiment shown in Fig. 3.

where k'_R is a positive design parameter. The limiting value is

$$L = -r\frac{bc}{(i_\mathrm{d} - \beta i_\mathrm{q})b - 2i_\mathrm{q}\hat{\omega}_\mathrm{m}} \tag{9}$$

where the parameter $0 < r < 1$ affects the stability margin of the system; choosing $r = 1$ would lead to a marginally stable system (in the operating points where k_R is determined by L).

In practice, the adaptation should be disabled in the vicinity of no-load operation and at higher frequencies due to poor signal-to-noise ratio (which is a fundamental property common to all stator-resistance adaptation methods based only on the fundamental-wave excitation). Hence, parameter k'_R in (8) can be selected as

$$k'_\mathrm{R} = \begin{cases} k''_\mathrm{R}\left(1 - \frac{|\hat{\omega}_\mathrm{m}|}{\omega_\Delta}\right)|i_\mathrm{q}|, & \text{if } |i_\mathrm{q}| > i_\Delta \text{ and } |\hat{\omega}_\mathrm{m}| < \omega_\Delta \\ 0, & \text{otherwise} \end{cases} \tag{10}$$

where k''_R, ω_Δ, and i_Δ are positive constants.

IV. Experimental Setup and Parameters

The operation of the observer and stator-resistance adaptation at low speeds was investigated experimentally using the setup shown in Fig. 2. The motion-sensorless control system was implemented in a dSPACE DS1104 PPC/DSP board. A 6.7-kW two-pole SyRM is fed by a frequency converter that is controlled by the DS1104 board. The rated values of the SyRM are: speed 3175 r/min; frequency 105.8 Hz; line-to-line rms voltage 370 V; rms current 15.5 A; and torque 20.1 Nm. The base values for angular speed, voltage, and current are defined as $2\pi \cdot 105.8$ rad/s, $\sqrt{2/3} \cdot 370$ V, and $\sqrt{2} \cdot 15.5$ A, respectively.

A servo induction motor is used as a loading machine. The rotor speed ω_m and position ϑ_m are measured using an incremental encoder for monitoring purposes. The shaft torque T_m is measured using a Dataflex 22 torque measuring shaft. The total moment of inertia of the experimental setup is 0.015 kgm^2 (2.7 times the inertia of the SyRM rotor).

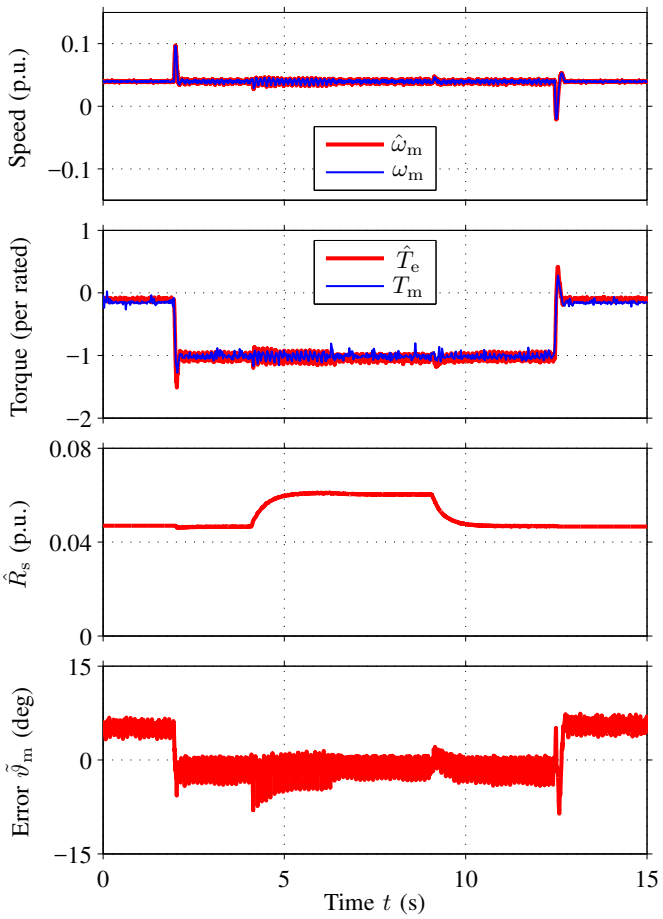

Fig. 3. Experimental results showing the stepwise increase of 0.2 Ω in the actual stator resistance at $t = 4$ s and the decrease at $t = 9$ s. The speed reference is kept at 0.04 p.u. and a negative rated load torque is applied at $t = 2$ s.

The stator resistance of the SyRM is approximately 0.65 Ω at room temperature. Additional 0.2-Ω resistors were added between the frequency converter and the SyRM. The resistance can be changed stepwise by opening or closing a manually operated three-phase switch (S) connected in parallel with the resistors. Unless otherwise noted, switch S is in the closed position.

The block diagram of the speed-sensorless control system implemented in the DS1104 board is shown in Fig. 1. The stator currents and the DC-link voltage are measured, and the reference voltage obtained from the current controller is used for the observer. The sampling is synchronized to the modulation, and both the switching frequency and the sampling frequency are 5 kHz. A simple current feedforward compensation for dead times and power device voltage drops is applied. The control system shown in Fig. 1 is augmented with a speed controller, whose feedback signal is the speed estimate $\hat{\omega}_\mathrm{m}$ obtained from the proposed observer. The bandwidth of this PI controller, including active damping [15], is $2\pi \cdot 5.3$ rad/s (0.05 p.u.). The estimate of the per-unit electromagnetic torque is evaluated as $\hat{T}_\mathrm{e} = (L_\mathrm{d} - L_\mathrm{q})i_\mathrm{d}i_\mathrm{q}$.

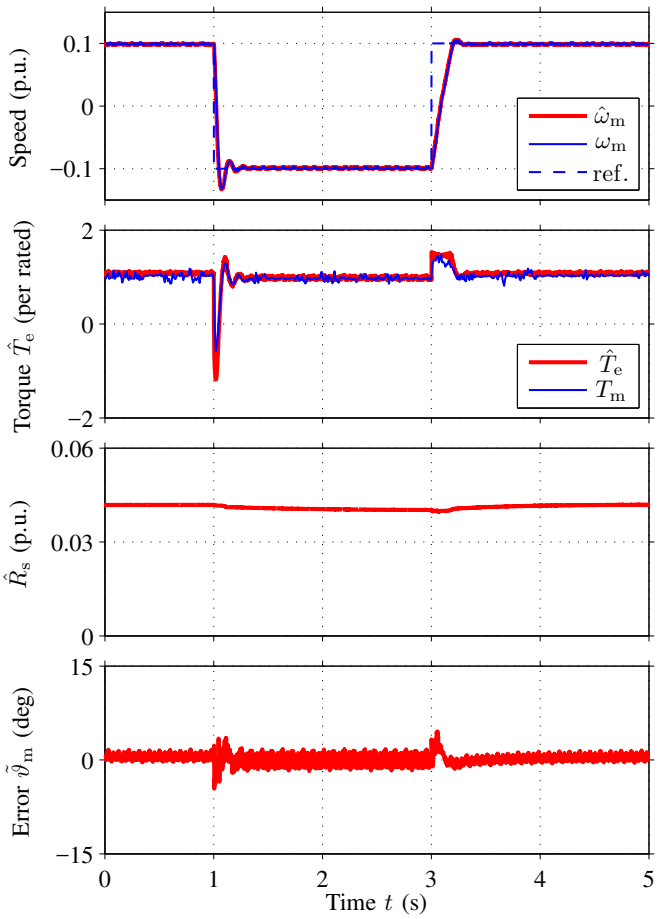

Fig. 4. Experimental results showing speed-reference steps (0.1 p.u. $\rightarrow -0.1$ p.u. $\rightarrow$ 0.1 p.u.) at rated load.

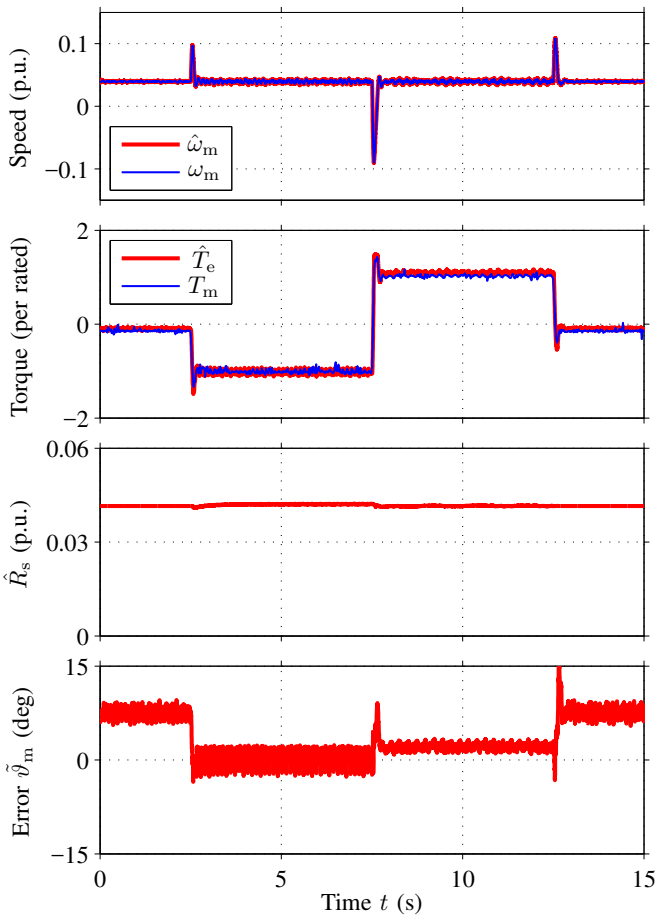

Fig. 5. Experimental results showing load-torque steps (0 negative rated $\rightarrow$ rated $\rightarrow$ 0) when the speed reference is kept at 0.04 p.u

The observer was implemented in the estimated rotor coordinates using (2), (5), (6), (8), and (10). The observer gain (5) is determined by the constant $b = 2$ p.u. The per-unit parameter estimates used in the experiments are: $L_\mathrm{d} = 2.20$ p.u. and $L_\mathrm{q} = 0.31$ p.u., and the d-axis current reference was 0.35 p.u. The parameters needed for the stator-resistance adaptation are: $r = 0.1$ in (9) and $k''_\mathrm{R} = 0.005$ p.u., $\omega_\Delta = 0.15$ p.u., and $i_\Delta = 0.2$ p.u. in (10).

V. Experimental Results

Fig. 3 shows the stepwise change in the stator resistance (as seen by the frequency converter). Initially, three-phase switch S, cf. Fig. 2, was in the closed position. The speed reference was kept at 0.04 p.u. A load torque step to the negative rated value was applied at $t = 2$ s. Switch S was opened at $t = 4$ s, causing a 0.014-p.u. increase (corresponding to 30%) in the actual stator resistance. Switch S was closed again at $t = 9$ s. It can be seen that the stator-resistance estimate tracks the change in the actual stator resistance.

Fig. 4 shows speed-reference steps under the rated load torque. The speed reference was stepped from 0.1 to -0.1 p.u. and then back to 0.1 p.u. Fig. 5 shows load-torque steps when the speed reference was kept at 0.04 p.u. The load torque was stepped to the negative rated value at $t = 2.5$ s, reversed at $t = 7.5$ s, and removed at $t = 12.5$ s. It can be seen that the observer behaves well both in speed and torque transients.

Results of a slow load-torque reversal are shown in Fig. 6. The speed reference was kept at 0.05 p.u. It can be seen that the torque estimate corresponds very well to the actual measured torque. The changes in the position error and in the estimated stator resistance suggest that the inductances are not well-tuned. In SyRMs, the d-axis flux component usually saturates strongly as a function of the corresponding current component. Furthermore, the d-axis saturation is coupled with the q-axis saturation [16].

Results of a slow speed reversals are shown in Fig. 7. A load torque step to the rated value was applied at $t = 2$ s. The speed reference was slowly ramped from 0.08 p.u. to -0.08 p.u. and back to 0.08 p.u. During the sequence, the drive operates in the motoring and regenerating modes. Without the stabilizing observer gain, this kind of speed reversals would not be possible. Furthermore, without the stator-resistance adaptation, a very accurate stator-resistance estimate would be needed since the frequency remains in the vicinity of zero for a long time.

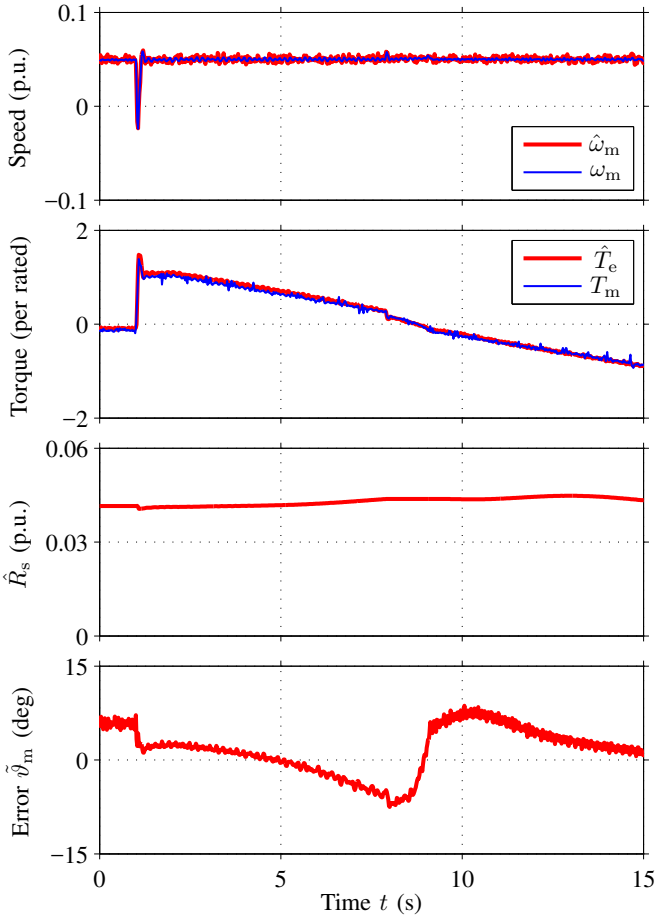

Fig. 6. Experimental results showing slow torque reversal when the speed reference is kept at 0.05 p.u.

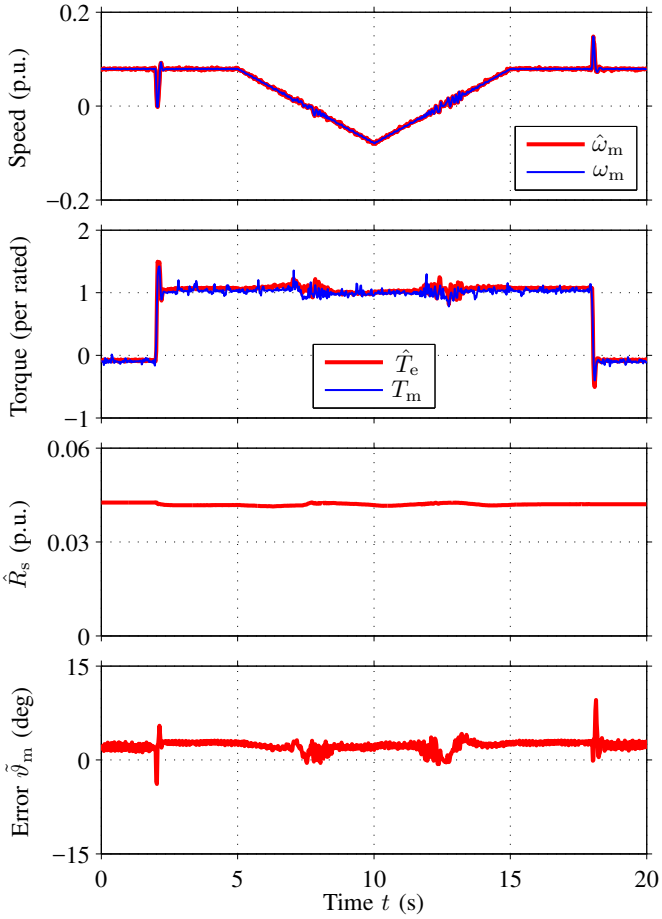

Fig. 7. Experimental results showing slow speed reversals (0.08 p.u. $\rightarrow$ -0.08 p.u. $\rightarrow$ 0.08 p.u.) when the rated load torque is applied.

VI. Conclusions

In this paper, a reduced-order position observer with stator-resistance adaptation was applied for motion-sensorless SyRM drives. If the inductances are known accurately, the position and stator-resistance estimation is stable at every operating point except the zero frequency. The observer design is simple, and it results in a comparatively robust and well-damped closed-loop system. The observer was experimentally tested using a 6.7-kW SyRM drive; stable operation at low speeds under different loading conditions is demonstrated. Constant inductance values were used in the experiments. It is assumed that using an inductance model should further improve the performance of the drive.

Acknowledgment

The authors gratefully acknowledge ABB Oy and the Academy of Finland for the financial support.

References

[1] A. Boglietti and M. Pastorelli, "Induction and synchronous reluctance motors comparison," Orlando, FL, Nov. 2008, pp. 2041–2044.

[2] E. Capecchi, P. Guglielmo, M. Pastorelli, and A. Vagati, "Position-sensorless control of the transverse-laminated synchronous reluctance motor," *IEEE Trans. Ind. Appl.*, vol. 37, no. 6, pp. 1768–1776, Nov./Dec. 2001.

[3] H. F. Hofmann, S. R. Sanders, and A. EL-Antably, "Stator-flux-oriented vector control of synchronous reluctance machines with maximized efficiency," *IEEE Trans. Ind. Electron.*, vol. 51, no. 5, pp. 1066–1072, Oct. 2004.

[4] R. Lagerquist, I. Boldea, and J. Miller, "Sensorless control of the synchronous reluctance motor," *IEEE Trans. Ind. Appl.*, vol. 30, no. 3, pp. 673–682, 1994.

[5] M. Jansson, L. Harnefors, O. Wallmark, and M. Leksell, "Synchronization at startup and stable rotation reversal of sensorless nonsalient PMSM drives," *IEEE Trans. Ind. Electron.*, vol. 53, no. 2, pp. 379–387, Apr. 2006.

[6] S. Koonlaboon and S. Sangwongwanich, "Sensorless control of interior permanent-magnet synchronous motors based on a fictitious permanent-magnet flux model," in *Conf. Rec. IEEE-IAS Annu. Meeting*, Hong Kong, Oct. 2005, pp. 311–318.

[7] S. Sangwongwanich, S. Suwankawin, S. Po-ngam, and S. Koonlaboon, "A unified speed estimation design framework for sensorless ac motor drives based on positive-real property," in *Proc. PCC-Nagoya'07*, Nagoya, Japan, Apr. 2007, pp. 1111–1118.

[8] J.-I. Ha, S.-J. Kang, and S.-K. Sul, "Position-controlled synchronous reluctance motor without rotational transducer," *IEEE Trans. Ind. Appl.*, vol. 35, no. 6, pp. 1393–1398, Nov./Dec. 1999.

[9] A. Consoli, F. Russo, G. Scarcella, and A. Testa, "Low- and zero-speed sensorless control of synchronous reluctance motors," *Electr. Power Comp. Syst.*, vol. 35, no. 5, pp. 1050–1057, Sep./Oct. 1999.

[10] T. Matsuo and T. A. Lipo, "Rotor position detection scheme for

synchronous reluctance motor based on current measurements," *IEEE Trans. Ind. Appl.*, vol. 31, no. 4, pp. 860–868, July/Aug. 1995.

[11] M. G. Jovanović, R. E. Betz, and D. Platt, "Sensorless vector controller for a synchronous reluctance motor," *IEEE Trans. Ind. Appl.*, vol. 34, no. 2, pp. 346–354, March/Apr. 1998.

[12] P. Guglielmi, M. Pastorelli, G. Pellegrino, and A. Vagati, "Position-sensorless control of permanent-magnet-assisted synchronous reluctance motor," *IEEE Trans. Ind. Appl.*, vol. 40, no. 2, pp. 615–622, Mar./Apr. 2004.

[13] M. Hinkkanen, T. Tuovinen, L. Harnefors, and J. Luomi, "A reduced-order position observer with stator-resistance adaptation for PMSM drives," in *Proc. IEEE ISIE'10*, Bari, Italy, July 2010, in press.

[14] A. Piippo, M. Hinkkanen, and J. Luomi, "Sensorless control of PMSM drives using a combination of voltage model and HF signal injection," in *Conf. Rec. IEEE-IAS Annu. Meeting*, vol. 2, Seattle, WA, Oct. 2004, pp. 964–970.

[15] L. Harnefors, "Design and analysis of general rotor-flux-oriented vector control systems," *IEEE Trans. Ind. Electron.*, vol. 48, no. 2, pp. 383–390, Apr. 2001.

[16] P. Guglielmi, M. Pastorelli, and A. Vagati, "Impact of cross-saturation in sensorless control of transverse-laminated synchronous reluctance motors," *IEEE Trans. Ind. Electron.*, vol. 53, no. 2, pp. 429–439, Apr. 2006.